67º congresso 2012 abm
67th abm international congress
ISSN 1516-392X

WELDING CHARACTERISTICS OF CORROSION RESISTANT NI-BASED ALLOYS MONEL 400 AND HASTELLOY C-276 THIN FOIL WELDED BY PULSED ND:YAG LASER[1]

Vicente A. Ventrella[2]
José Roberto Berretta[3]
Wagner de Rossi[3]

Abstract
In this paper a Nd:YAG pulsed laser beam was used to join Monel 400 and Hastelloy C-276 thin foils, and the effects of pulse energy on the quality of the welding joints characteristics were analyzed. Pulsed laser processing is expected to be the method of choice because it allows more precise heat control compared with arc and plasma processing. Welding thin foils is very important in many industrial applications. The need for joints between different thicknesses often appears in complex components, especially the combination with a more corrosion resistant material. Due to differences in thermal conductivity, fusion temperature and solubility of the materials, brittle phases can appear and deteriorate the tensile strength of the joint. Pulsed laser systems have the capability to weld thin foils without filler metal (autogenous welding), high energy density and low heat-input. The pulse energy was varied from 1.0 J to 2.25 J at an increment of 0.25 J and a 4 ms pulse duration. The macro and microstructures of the welds were analyzed by optical microscopy. Sound laser welds without discontinuities were obtained with 1.5 J and 1.75 J pulse energy. Results indicate that using a precise control of the pulse energy, and so a control of the dilution rate, is possible to weld Monel 400 and Hastelloy C-276 thin foils by pulsed Nd:YAG laser.
Key words: Laser welding; Nd:YAG; Monel 400; Hastelloy C-276.

[1] *Technical contribution to 67th ABM International Congress, July, 31th to August 3rd, 2012, Rio de Janeiro, RJ, Brazil.*
[2] *Depto. de Eng. Mecânica, Universidade Estadual Paulista (Unesp), SP, Brasil; ventrella@dem.feis.unesp.br*
[3] *Instituto de Pesquisas Energéticas e Nucleares (IPEN), Centro de Lasers e Aplicações, SP, Brasil.*

ISSN 1516-392X

1 INTRODUCTION

Laser is one of the highest power density sources available to industry today. It is similar in power density to an electron beam. Laser processes represent part of the new technology of high-energy-density processing. A basic laser consists of two mirrors which are placed parallel to each other to form an optical oscillator, that is, a chamber in which light travelling down the optic axis between the mirrors, and where there is an active medium which is capable of amplifying the light oscillations by the mechanism of stimulated emission. There is also some system for pumping the active medium so that it has the energy to become active. Lasers generate light energy that can be absorbed into materials and converted to heat energy. Because of high power density of the laser beam, laser welding is characterized by very narrow fusion zone, narrow weld width and high penetration.[1]

Monel 400, an important nickel-copper alloy, and Hastelloy C-276, a nickel-based alloy with high concentrations of Cr and Mo, are more corrosion resistant than stainless steels. This characteristic together with their good ductility and easy of cold working make them generally very attractive for a wide variety of applications; nearly all of which exploit their corrosion resistance in atmospheric, salt water and various acid and alkaline media. The alloys are used for marine engineering, chemical and hydrocarbon processing equipment, valves, pumps, sensors and heat exchangers. Nickel and cooper, the principal constituent metals of the alloy are less corrosion resistant than Monel 400 under reducing and oxidizing conditions, respectively.[2]

Welding thin foil materials is very important in many industrial applications. The need for joints between thin foils often appears in complex components, especially the combination with a more corrosion resistant material. Due to differences in thermal conductivity, fusion temperature and solubility of the materials, brittle phases can appear and deteriorate the tensile strength of the joint. Pulsed laser systems have the capability to weld different materials without filler metal (autogenous welding), high energy density and low heat-input. Industrial components are being made smaller to reduce energy consumption and save space, which creates a growing need for microwelding of thin foil less than 100 μm thick. For this purpose, laser processing is expected to be the method of choice because it allows more precise heat control compared with arc and plasma processing.[3]

Welding with pulsed Nd:YAG Laser System is characterized by periodic heating of the weld pool by a high peak power density pulsed laser beam incident that allow melting and solidification to take place consecutively. However, due to very high peak power density involved, the solidification time is shorter than continuous laser and conventional welds. Combination of process parameters such as pulse energy [E_p], pulse duration [t_p], repetition rate [R_r], beam spot size [Φ_b] and welding speed [v] determines the welding mode, that is, conduction or keyhole.[4-6]

Research examining the Nd:YAG laser for continuous welding, pulsed welding, dissimilar sheet welding and coated sheet welding has been published. Kim et al.[7] reported successful welding of Inconel 600 tubular components of nuclear power plant using a pulsed Nd:YAG laser. Ventrella et al.[8] using a homemade Nd:YAG Pulsed Laser System studied thin foil welding of austenitic stainless steel. Ping and Molian[9] utilized a nanosecond pulsed Nd:YAG laser system to weld 60 μm of thin AISI 304 stainless steel foil.

The present work has been carried out to investigate the influence of the pulse energy on neodymium: yttrium aluminum garnet (Nd:YAG) laser welding of nickel-

ISSN 1516-392X

based alloys couples of Monel 400 and Hastelloy C-276 thin foil and its effect on weld joint characteristics.

2 EXPERIMENTAL

This study used a pulsed Nd:YAG laser system. The experimental setup of the laser system is shown in Figure 1.
Monel 400 and Hastelloy C-276 with thickness of 100 μm was used as base metal. Table 1 and Table 2 show the detail chemical compositions of the base metal, respectively. Before welding, the specimens were prepared and cleaned to ensure that all samples presented the same surface conditions with a homogeneous finish.

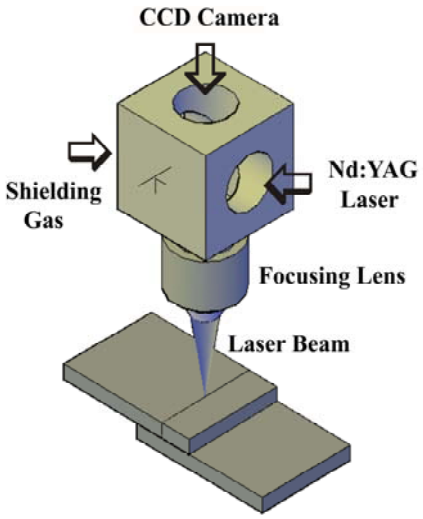

Figure 1. Experimental setup of the laser system.

Table 1. Chemical composition of Monel 400 (wt %)

Type	Ni	Cu	Fe	Si	Mn	C	S
Monel 400	65	Rem.	2.5	0.50	2.0	0.30	0.024

Table 2. Chemical composition of Hastelloy C-276 (wt %)

Elements	C	Cr	Ni	Mn	Si	Mo	Co	W	Fe
Hastelloy C-276	0,01	15,88	Bal	0,52	0,03	15,64	1,51	3,38	5,35

To evaluate the influence of the pulse energy, welding was performed using specimens of Monel 400 and Hastelloy C-276 positioned as similar lap joints. Both materials were welded with the same conditions and a beam spot size (Φ_b) and beam angle (A_b) of 0.2 mm and 90 degrees, respectively. The focus point was fixed on the surface of the work-piece. The welding speed (υ) and repetition rate (R_r) were fixed at 525 mm/min and 39 Hz, respectively. The pulse energy (E_p) varied from 1.0 to 2.25 J at increments of 0.25 J with a 4 ms pulse duration (t_p). Thus, there was one controlled parameter in this process: the pulse energy. The specimens were held firmly using a jig, to fixture and prevent absence of contact and excessive distortion, as shown in Figure 2. Fixturing is extremely important for thin-section laser welding. Tolerances were held closely to maintain joint fitups without allowing either mismatch or gaps.

ISSN 1516-392X

The specimens were laser-welded in an argon atmosphere at a flow rate (F_r) of 12 l/min. Back shielding of the joint was not necessary because Ni-based alloys Monel 400 and Hastelloy C-276 are not oxidizable metals like Al and Ti. None of the specimens were subjected to any subsequent form of heat treatment or machining. After welding, the specimens were cut for the tensile-shear tests (Figure 3).

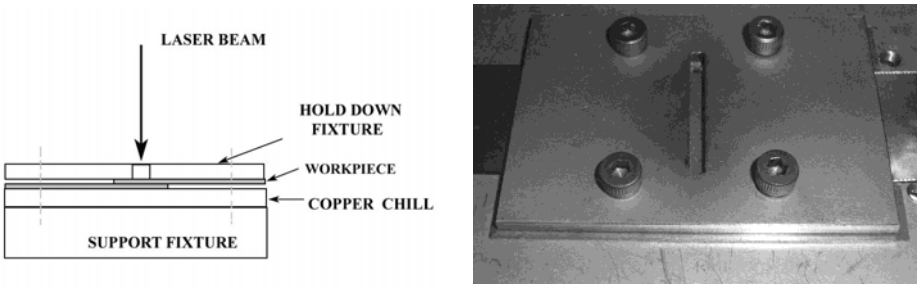

Figure 2. Schematic of the hold-down fixture developed to hold the thin foils.

Finally, part of the cut surfaces was prepared for metallographic inspection by polishing and etching to display a bead shape and microstructure. Metallographic samples were prepared with a solution of 50% nitric acid and 50% acetic acid. And Hastelloy C-276 samples with a solution of Metallographic samples were prepared with a solution of 40 ml hydrochloric acid, 2 ml nitric acid, 0.5 g copper chloride and 10 ml glycerol. The bead shape measurements were made using an optical microscope with an image analysis system. Figure 4 shows a schematic illustration of the transverse joint section with the analyzed geometric parameters.

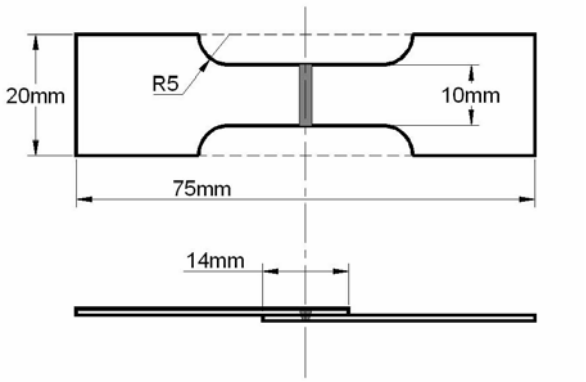

Figure 3. Schematic diagram of tensile test specimen design.

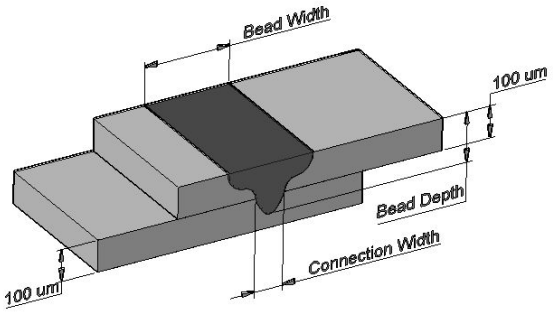

Figure 4. Joint transversal section showing the analyzed geometric parameters [mm].

ISSN 1516-392X

The strength of the welds was evaluated using Vickers microhardness and tensile shear strength tests. Microhardness tests were performed on a transverse section of the weld bead, parallel to the surface of the thin foils, in the region next to the connection line of the top foil. Microhardness tests identify possible effects of microstructural heterogeneities in the fusion zone and in the base metal. The reported data were the average of five individual results. For the tensile shear test, specimens were extracted from welded samples, and the width of the samples was reduced to 10 mm to lower the load required to fracture them.

3 RESULTS

Figure 5a shows Monel 400 welded sample with 1.5 J pulse energy after the tensile shear test and Figure 5b a top view of the weld bead. The cross section macrostructures of Monel 400 and Hastelloy C-256 lap laser welds as a function of pulse energy (E_p) are summarized in Figures 6 and 7, respectively. In Figures 6a and 7a (specimen with 1.0 J pulse energy) no penetration at the bottom sheet and no depression at the top of the bead was observed, probably due to insufficient laser energy to bridge the couple. Due to the thin thickness, low pulse energy of the laser beam and the presence of a small gap, the molten pool just grew in the radial direction of the top foil resulting in a no bonded joint with the weld morphology observed in Figures 6a and 7a. Gaps between foils and gaps in the connection line increase stress and thus are detrimental to weld quality in terms of mechanical properties. When the pulse energy was increased on the other specimens, a connection region between the foils was observed, as shown in Figures 6b to 6f and Figures 7b to 7f. In Monel 400 and Hastelloy C-276 specimens, welded with 2.25 J pulse energy, an increase occurred with a depression at the top and a penetration bead. The concavity increased proportionally to the pulse energy (E_p). Moreover, it was evident that specimens welded with 2.0 and 2.25 J pulse energy undergo deformation during joint welding, which causes a large bending moment. Areas near the heat source of the upper foil are heated to higher temperatures and thus expand more than areas away from the heat source or regions of the lower foil. After the foil cools to the initial temperature, the final deformation remains. Like the material heated by the laser beam, the irradiance did not cause the material reach its boiling point; no significant amount of surface material was removed.

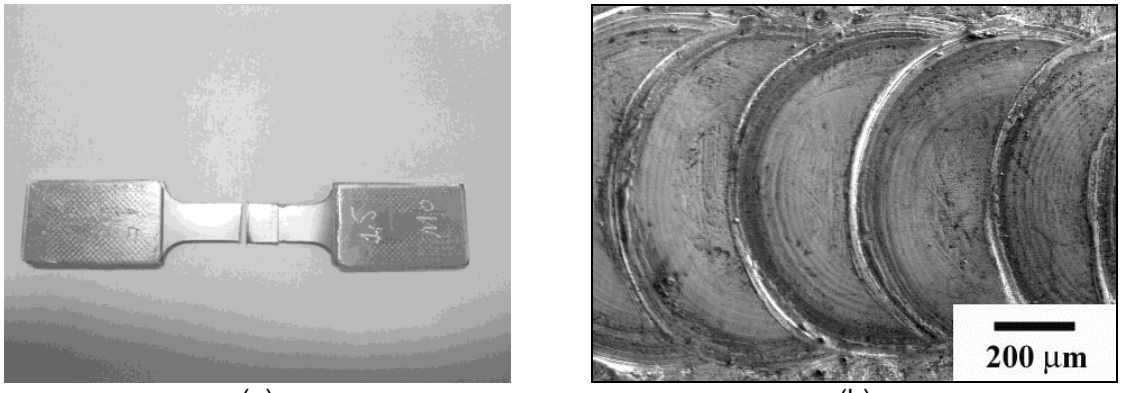

(a) (b)

Figure 5. Welded specimen after the tensile shear test (a) and a pulsed weld bead (b).

ISSN 1516-392X

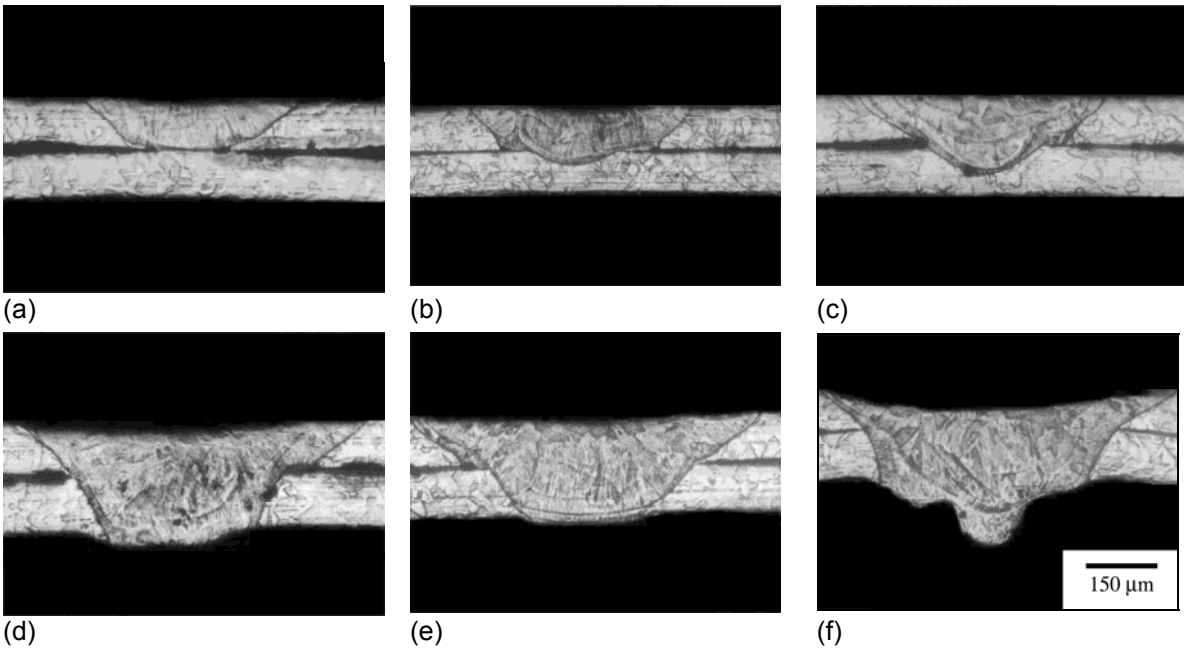

Figure 6. Cross sections of Monel 400 lap joints made with pulsed Nd:YAG laser welding with different pulse energies (E_p): a) 1.0 J, b) 1.25 J, c) 1.50 J, d) 1.75 J, e) 2.0 J and f) 2.25 J. All figures have the same magnification as shown in (f).

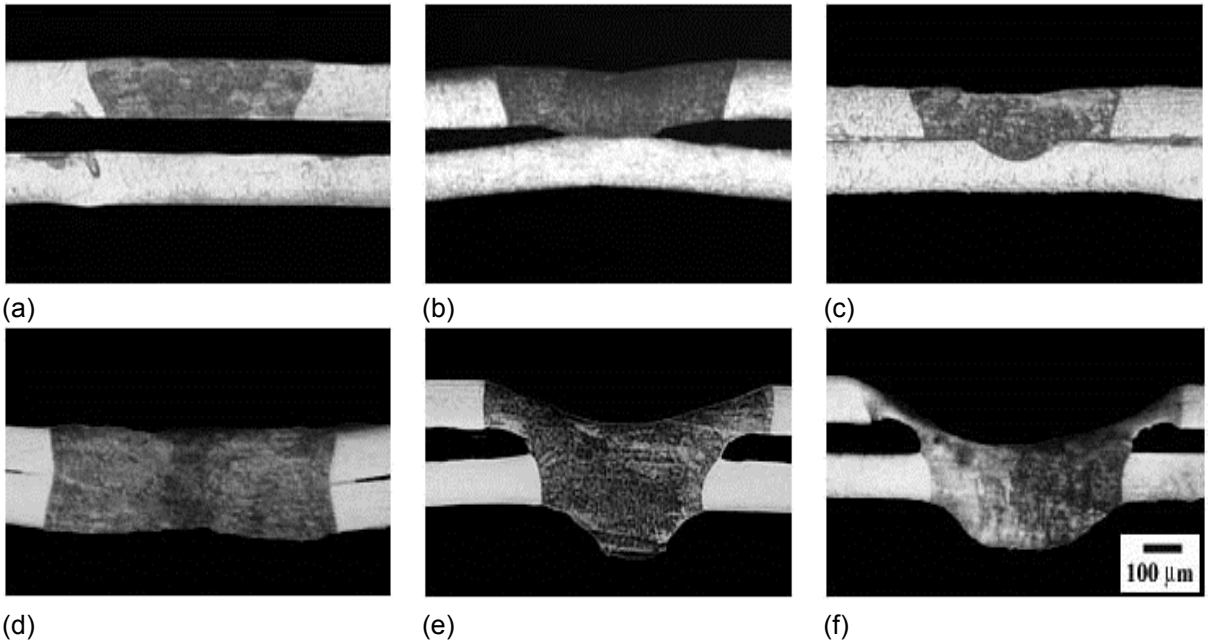

Figure 7. Cross sections of Hastelloy C-276 lap joints made with pulsed Nd:YAG laser welding with different pulse energies (E_p): a) 1.0 J, b) 1.25 J, c) 1.50 J, d) 1.75 J, e) 2.0 J and f) 2.25 J. All figures have the same magnification as shown in (f).

ISSN 1516-392X

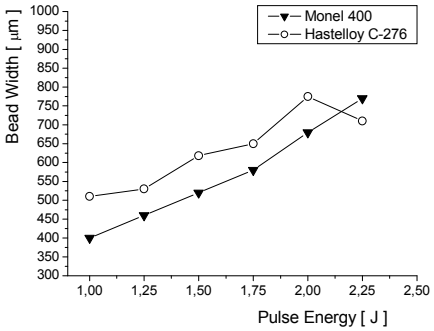

Figure 8. Bead width as a function of pulse energy [E_p].

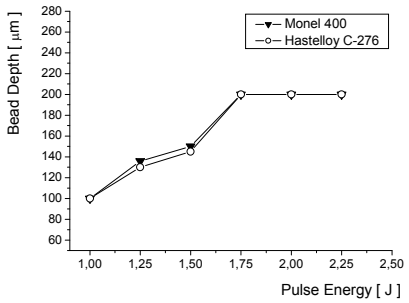

Figure 9. Bead depth as a function of pulse energy [E_p].

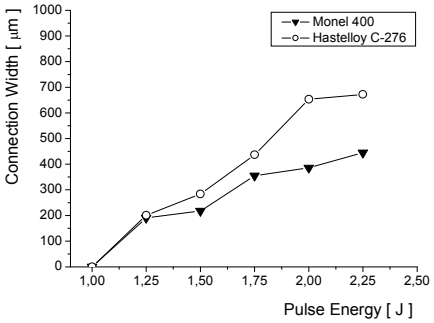

Figure 10. Connection width as a function of pulse energy [E_p].

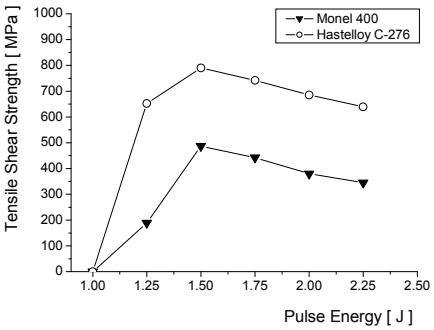

Figure 11. Relationship between pulse energy and tensile shear strength.

The tensile properties of the welded joint affected by pulse energy (Ep) can be explained by macro and microstructural analyses. When the pulse energy is too low, the welding molten pool has not enough time to form, and incomplete penetration is

ISSN 1516-392X

formed. As the pulse energy increases, the grains in the weld metal and in the HAZ become coarser. The heat-affected zone extension increases too. Discontinuities become more severe. Some precipitates can be present intergranularly and even continuously along the grain boundary. These microstructures changes contribute to a weakness of the weld joint, which reduces the tensile properties as reported in the literature.[10] Finally, the decrease in the UTS may be related to the change of the microstructures and HAZ extension. Therefore, based on the above analyses it can be concluded that the lower the pulse energy, provided complete penetration occurs, the higher the tensile properties of welded joints.

Hardness profiles of the base metal, heat-affected zone and weld metal of AISI 316L stainless steel thin foils as a function of pulse energy are shown in Fig. 11. No significant difference between hardness of weld metal and the heat-affected zone was obtained; the hardness of the heat-affected zone was slightly higher than that of the weld metal regardless of the pulse energy. Base metal hardness was always lower than that of HAZ and weld metal. These results are valid for all joints. This is expected because the mechanical properties of steel, in general, are based on its microstructures.[11]

Figure 12 illustrates typical microstructures of Monel 400 weld joint. Figure 12a shows the fusion line solidification structure at the top of the weld where the un-melted base metal grains act as substrates for nucleation of the fusion zone columnar grains (epitaxial growth), which are perpendicular to the fusion boundary. Figure 12b shows the heat affected zone at the bottom of the joint where the effects of the large thermal gradient in this region are evident. Comparing thin and thick foil welding, it can be concluded that the grains in the solid state coarsen with decreasing parent metal thickness. This shows that the volume of the parent metal plays an important role during the welding thermal cycle. As the material volume decreases, the time to cooling increases and the heat-affected zone appearance coarsens. This indicates that in thin foil welding, heat-affected zone control is of considerable importance for welded joint quality.

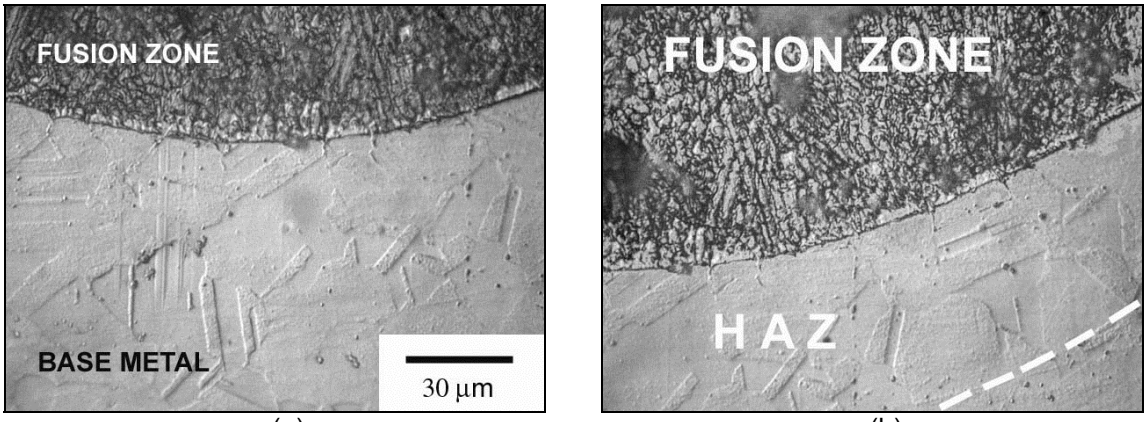

(a) (b)

Figure 12. Typical optical microstructures of the fusion zone (a) and heat-affected-zone of Monel 400 welded joint (1,5 J). Both figures have the same magnification as shown in (a).

As can be seen in Figure 11, the microhardness values (HV10) decreased as the joint energy increased (1.0 J to 2.25J) to maximum energy (2.25 Joules). During the solidification of the fusion zone, the material generally loses original strength that is induced by strain hardening. Microhardness profiles in welded joints obtained with lower energy show increasing of the hardness in the fusion zone and a finer microstructure that is induced by rapid cooling.

ISSN 1516-392X

4 DISCUSSION

The macroscopic examination of the cross sections of all specimens also indicated that the weld pool morphology is essentially symmetrical about the axis of the laser beam. A hemispherical weld bead was formed in a similar manner to conventional arc fusion welding processes. This symmetry at the top and bottom was observed in all joints independent of the pulse energy, which suggests a steady fluid flow in the weld pool; however, as the pulse energy increased, a high depression formed at the top.

Liao and Yu[12] and Manonmani et al.[13] reported that, in pulsed laser welding with the same incident angle of AISI 304 stainless steel the characteristic lengths of the weld increased as the laser energy increased. The same tendency was observed in the present work as the pulse energy increased to 2.0 J. With pulse energy greater than 2.0 J, excessive burnthrough occurred and an excess of melt material at the root region was observed. This reduced the radial conductive heat transfer at the top foil, and the bead width decreased slightly, as shown in Figure 6f.

These macrostructural results indicate that weld metal characteristics are sensitive to pulse energy variation. To obtain an acceptable weld profile, intimate contact between couples is necessary. The presence of an air gap in the weld joint restringes heat transfer between the workpieces. This results in a lack of fusion of the bottom element or the formation of a hole on the superior element of the joint. As the pulse energy increases, the concavity at the top of the weld and the excess of material at the weld root increase; consequently, the weld joint is weakened. Moreover, higher pulse energy extended the heat-affect zone.

In summary, the most acceptable Monel 400 and Hastelloy C-276 weld beads were obtained at pulse energy of 1.5 and 1.75 joules, where the molten pool bridged the couple and the weld bead profile showed minimum underfill. The maximum depth (full penetration) was observed at pulse energy of 1.75 joules and the maximum tensile shear test exhibited 487 MPa to Monel 400 and 790 MPa to Hastelloy C-276. No undercut and minimum porosity were observed. No evidence of hot cracking was observed in the weld metal and this is attributed to the rapid solidification conditions typical of the pulsed Nd:YAG laser welding process.

5 CONCLUSION

The results obtained from this study demonstrate that is possible to weld 100 μm thickness of Monel 400 and Hastelloy C-276 thin foils, in terms of microstructural and mechanical reliability, by precisely controlling the laser pulse energy. The better performance was due to the high quality joint; a joint marked by good penetration, no underfill and free from microcracks and porosity. This was obtained at an energy pulse of 1.5 J, a repetition rate [R_r] of 39 Hz and a 4 ms pulse duration. This reflects one of the most notable features of pulsed laser welding compared with other processes; welding with low heat input. The work also shows that the process is very sensitive to the gap between couples which prevents good heat transfer between the foils. The shape and dimensions of the thin foil weld bead observed in the present work depended not only on the pulse energy, but also on the presence of gaps between foils. Bead width, connection width and bead depth increased as the pulse energy increased. The ultimate tensile strength (UTS) of the welded joints initially increased and then decreased as the pulse energy increased. The specimen welded with 1.5 J attained the maximum tensile shear strength. In all the specimens, fracture

ISSN 1516-392X

occurred in the top foil heat-affected zone next to the fusion line. The microhardness was almost uniform across the parent metal, HAZ and weld metal. A slight increase in the fusion zone compared to those measured in the base metal was observed. This is related to the microstructural refinement in the fusion zone, induced by rapid cooling.

Acknowledgements

The authors gratefully acknowledge the financial support of CNPq.

REFERENCES

1 Bertolotti, M.; Masers and Lasers, Bristol:Adam Hilger, 1983.
2 SINGH,V.B.; GUPTA, A.: The electrochemical corrosion and passivation behavior of Monel 400 in concentrated acids and their mixtures. In: Journal of Materials Science, 36 (2001), pp. 1433-1442.
3 ABE, N., FUNADA, Y., IMANADA, T., TSUKAMOTO,M., Microwelding of thin stainless steel foil with a direct diode laser. Transaction of JWRI, 34, p.19-23, 2005
4 ION, J.C., Laser Processing of Engineering Materials, UK, Ed. Elsevier, 2005.
5 DULEY, W.W., Laser Welding, USA, Ed.John Wiley&Sons, 1999.
6 STEEN, W.M., 2005, Laser Material Processing, USA, Springer, 2005.
7 KIM, D.J.; KIM, C.J. AND CHUNG, C.M. , Repair welding of etched tubular components of nuclear power plant by Nd:YAG laser. Journal of Materials Processing Technology, 14, p.51-56, 2001.
8 VENTRELLA, V.A.; BERRETTA, J.R.; ROSSI, W. , Pulsed Nd:YAG laser seam welding of AISI 316L stainless steel thin foils. Journal of Materials Processing Technology, 210, p. 1838-1843, 2010.
9 PING, D. AND MOLIAN,P., Q-switch Nd:YAG laser welding of AISI stainless steel foils. Materials Science & Engineering A, 486, p.680-685, 2008.
10 QUAN,Y.J., CHEN,Z.H., GONG,X.S., YU,Z.H., Effects of heat input on microstructure and tensile properties of laser welded magnesium alloy AZ31. Materials Characterization, 59, p.1491-1497, 2008.
11 ABDEL, M.B., Effect of laser parameters on fusion zone shape and solidification structure of austenitic stainless steels. Materials Letters 32, p.155-163, 1997.
12 LIAO, Y. AND YU, M. Effects of laser beam energy and incident angle on the pulse laser welding of stainless steel thin sheet. Journal of Materials Processing Technology 190, p.102-108, 2007.
13 MANONMANI, K., MURUGAN,N. AND BUVANASEKARAN,G. Effects of process parameters on the bead geometry of laser beam butt welded stainless steel sheets. International Journal of Advanced Manufacturing Technology, 32, p.1125-1133, 2007.